Materials and Design 32 (2011) 815–821

Contents lists available at ScienceDirect

Materials and Design

journal homepage: www.elsevier.com/locate/matdes

Design of lightweight multi-material automotive bodies using new material performance indices of thin-walled beams for the material selection with crashworthiness consideration

Xintao Cui [a], Hongwei Zhang [b], Shuxin Wang [b], Lianhong Zhang [b], Jeonghan Ko [c,*]

[a] Tianjin FAW Xiali Automotive Co., Ltd., Tianjin 300190, PR China
[b] School of Mechanical Engineering, Tianjin University, Tianjin 300072, PR China
[c] Department of Industrial and Management Systems Engineering, University of Nebraska-Lincoln, Lincoln, NE 68588, USA

ARTICLE INFO

Article history:
Received 22 March 2010
Accepted 15 July 2010
Available online 17 July 2010

Keywords:
H. Performance indices
H. Value analysis
A. Multi-materials

ABSTRACT

Currently, automotive bodies are constructed usually using a single material, *e.g.* steel or aluminum. Compared to single-material automotive bodies, multi-material automotive bodies allow optimal material selection in each structural component for higher product performance and lower cost. This paper presents novel material performance indices and procedures developed to guide systematic material selection for multi-material automotive bodies. These new indices enable to characterize the crashworthiness performance of complex-shaped thin-walled beams in multi-material automotive bodies according to material types. This paper also illustrates the application of these performance indices and procedures by designing a lightweight multi-material automotive body. These procedures will help to design a lightweight and affordable body favored by the automotive industry, thus to reduce fuel consumption and greenhouse gas emissions.

1. Introduction

Vehicle weight reduction has been considered as one of the most important solutions to improve fuel economy and reduce harmful emissions. In recent years, there have been growing concerns over fuel consumption and pollution caused by the increasing number of automobiles, and the automotive industry is under great pressure to reduce fuel consumption and emissions. One solution to these problems is to reduce a vehicle's weight, because 57 kg weight reduction is equivalent to 0.09–0.21 km per liter fuel-economy increase [1]. This reduction is critical especially these days, as the fuel costs are rising and concerns on the climate change are growing.

It is believed that the vehicle body weight can be reduced by the use of multiple materials without cost increase. Various lightweight automotive bodies have been developed using high strength steels [2,3], aluminum alloys [4,5] and composite materials [6]. These special materials can provide lighter weight car bodies. However, the high prices of these special materials have been one of the main barriers to replacing steel with these materials [7]. Therefore, some studies [5,8–10] have argued that the multi-material car bodies are solutions to these problems.

The design of optimized multi-material automotive bodies requires novel material performance indices to effectively evaluate the advantages and disadvantages of using such multiple materials for complex-shape structural components. The concept of the multi-material use is that the right material types are used in the right locations for the desired product functions. Various methods have been developed for such material selection [11–13]. For example, Ashby' method [11] defines a material performance index, and then ranks materials based on the performance index to select the best one for the optimal design of beams, shafts, panels, etc. Many performance indices have been developed for structures with simple geometries. However, the structural beam components of automotive bodies such as A-pillars, B-pillars, cross members, rails and rail extensions do not have such simple structures. Therefore, there is a need to develop performance indices for more geometrically complex structures, which are usually common in automotive bodies.

Furthermore, in spite of their practical importance, material performance indices for automotive body assemblies have been addressed only in limited aspects of body performance. In general, the material selection problems were studied extensively. Several monographs describe general theories and procedures on material selection [11,14]. The role of knowledge-based material selection was described in the context of concurrent engineering [15]. Structural optimization was applied for the choice of materials considering the environmental impact of materials [16] and for

* Corresponding author. Tel.: +1 402 472 3495; fax: +1 402 472 1384.
E-mail address: jko2@unl.edu (J. Ko).

0261-3069/$ - see front matter © 2010 Elsevier Ltd. All rights reserved.
doi:10.1016/j.matdes.2010.07.018

material selection for a side rocker beam of a car body [17]. Some studies [12,13] proposed the material performance indices for stiff and light automotive body assemblies. These studies pioneered investigating the weight reduction by material substitution with constant stiffness. However, for more comprehensive body performance evaluation, further research is desirable to consider additional aspects of car body performance such as crashworthiness and material costs.

This paper presents novel performance indices and procedures to select materials for lightweight and cost-effective multi-material automotive bodies. These new indices can characterize the material performance of complex-cross-section and thin-walled structural beams in automotive bodies for crashworthiness design. The calculation procedures for the indices are also presented. This paper also presents methods to consider the material costs in the material selections. A case study applies these new performance indices and procedures to the design of a cost-effective lightweight automotive body of multi-material construction.

2. Performance index for crashworthiness design

This section presents material performance indices of thin-wall structural components having general cross-sections for the optimal material selection considering crashworthiness. In this study, the topology of the components is assumed to be given, but the thickness can be changed in material selection procedures.

2.1. Generalized formula of the mean crush load

In this section, a generalized formula is expressed for the mean crush road of a thin-walled beam. In the forward and rear sections located away from the passenger compartment, main crush-load carrying components are located and they are designed to absorb kinetic energy during collision. The mean crush load, F_m, is a widely accepted design parameter to evaluate the capability of thin-walled components to absorb crash energy [18]. F_m is defined as the ratio of energy absorption to the deformed length.

In analytical as well as experimental studies [19–21], the formulas for the mean crush load of simple thin-walled beams were developed in concise forms including component geometry parameters and material properties. Wierzbicki and Abramowicz [19] presented the mean crush load of a rectangular box column as

$$F_m = 38.27 M_0 B^{1/3} t^{-1/3} = 9.5675 B^{1/3} \sigma_f t^{5/3} \tag{1}$$

where $M_0 = \sigma_f t^2/4$ is the fully plastic moment, σ_f is the average flow stress, $B = (c + d)/2$ with c and d being the lengths of a rectangular box column, and t is the wall thickness. Guillow et al. [20] developed an axial crushing load formula of circular tubes by an experimental study as

$$F_m = 72.3 M_0 (D/t)^{0.32} = 18.075 D^{0.32} \sigma_f t^{1.68} \tag{2}$$

where D is the average tube diameter and t is the tube thickness. The expression for the mean crush load of top-hat structures [21] is

$$F_m = 52.2 M_0 (L/t)^{1/3} = 13.05 L^{1/3} \sigma_f t^{5/3} \tag{3}$$

where t is the wall thickness, and $L = 2w + 2h + 4f$ with h, w and f being the height of the hat-section, width of the hat-section and flange width, respectively.

In general, the plastic deformation energy depends on plastic tensile ($N_p = \sigma_f bt$) or plastic bending ($M_p = \sigma_f bt^2/4$), where b is the width of the cross-section. In addition, when thin-walled structures are under both plastic tensile load and plastic bending moment, the mean crush load F_m can be expressed as [21]

$$F_m \propto t^Q \tag{4}$$

where the exponent Q varies between 1 and 2.

As can be observed among the formulas above, if the topology and shape of a thin-walled beam is given, the mean crushing load F_m can be expressed as a function of the average flow stress and wall thickness as

$$F_m = C \sigma_f t^Q \tag{5}$$

where C is a constant, σ_f is the average flow stress and t is the wall thickness. The average flow stress σ_f is expressed as [22]

$$\sigma_f = (\sigma_Y + \sigma_U)/2 \tag{6}$$

where σ_Y and σ_U are the yield and ultimate stress, respectively.

2.2. Evaluation of the material indices for thin-walled structures

In this section, the material index for thin-walled general-shaped structures is developed to evaluate their mean crush load performance, and the calculation procedure is also presented.

Consider two components (beams) made of two different materials but having the same shape. Let subscript "1" refer to the reference material of the two materials and "2" the material under design consideration. If the two components have the same mean crush load, then from Eq. (5) the thickness of the component made of material M_2 is expressed as

$$t_2 = t_1 (\sigma_{f1}/\sigma_{f2})^{1/Q} \tag{7}$$

The mass of a thin-walled beam is

$$m = \rho A t \tag{8}$$

where A is the cross-sectional area of a beam, t is the beam wall thickness, and ρ is the material density.

Using Eq. (5) to replace t in Eq. (8) and re-arranging the equation, the mass of a thin-walled beam is represented by the crush load, material property and geometry parameters as

$$m = \left(\frac{F_m}{C}\right)^{1/Q} A \left(\frac{\rho}{\sigma_f^{1/Q}}\right) \tag{9}$$

For a predefined beam geometry and crush-load value, $(F_m/C)^{1/Q} A$ in Eq. (9) is constant. Thus, the appropriate (lightweight) materials are those having smaller values of $\rho/\sigma_f^{1/Q}$ in Eq. (9). In other words, the materials of a large performance index defined in Eq. (10) below will be more suitable.

$$M_c = \frac{\sigma_f^{1/Q}}{\rho} \tag{10}$$

The exponent Q in the performance index can be calculated as follows. Note that the exponent Q in Eqs. (5) and (10) cannot be calculated by a purely analytical approach for thin-walled complex geometries due to nonlinearity. Thus, finite element (FE) simulations can be used to obtain the mean crush load F, and Q can be calculated iteratively with the help of FE analysis.

Taking logs on both sides of Eq. (5)

$$\log(F_m) = \log(C \sigma_f t^Q) = \log(C \sigma_f) + Q \log(t) \tag{11}$$

From Eq. (11), for two different thickness values t' and t'' and for the same material, Q can be expressed as

$$Q = \frac{\log(F'_m) - \log(F''_m)}{\log(t') - \log(t'')} = \frac{\log(F'_m/F''_m)}{\log(t'/t'')} \tag{12}$$

where F'_m and F''_m denote the mean crush loads corresponding to t' and t'', respectively.

Several values of Q can be calculated using Eq. (12) with respect to various combinations of two thicknesses, and the average value can be taken as Q estimate. Note that the accuracy of Q numerical

calculation depends on the mean crush load accuracy from the FE simulations and t'/t'' ratio. Also, the bigger the difference between t' and t'' is, the more accurate Q estimation is, as describe below. Suppose that there is a thin-walled beam whose mean crushing force is F'_m and thickness is t'. Also assume that $\Delta F'_m$ is the error of the value of F'_m. Then the estimate of Q becomes

$$\hat{Q} = \frac{\lg[(F'_m + \Delta F'_m)/F''^m)]}{\lg(t'/t'')} = \frac{\lg[(1 + \Delta F'_m/F'_m)(F'_m/F''_m)]}{\lg(t'/t'')}$$
$$= \frac{\lg(1 + \Delta F'_m/F'_m)}{\lg(t'/t'')} + \frac{\lg(F'_m/F''_m)}{\lg(t'/t'')} = \frac{\lg(1 + \Delta F'_m/F'_m)}{\lg(t'/t'')} + Q \qquad (13)$$

Thus, the Q estimation error caused by the mean crush load error $\Delta F'_m$ is $\frac{\lg(1+\Delta F'_m/F'_m)}{\lg(t'/t'')}$. Fig. 1 shows an example of the Q estimate error caused by a 5% error of a mean crush load evaluation. When the value of t'/t'' is 1.1, the value of Q deviates by 0.5. When the value of t'/t'' is 1.6, the deviation diminishes to 0.1.

The exponent Q and index M_c are easy to evaluate and implement, because: (1) the equations are simple to use, and (2) the mean crush loads can be calculated easily from simple FE software using computer aided design (CAD) data.

3. Application of the performance indices for the material selection of individual components

This section describes how the performance index can be used to determine the material for individual components.

3.1. Consideration of stiffness

In general, the performance index for stiffness design of thin-walled structures can be defined as $E^{1/q}/\rho$ [12,13], where E is the elastic modulus, ρ is the material density and q is an exponent. Ashby [11] has classified performance indices for beam stiffness into three categories depending on design purposes: (1) $E^{1/2}/\rho$ for cross-section area, (2) E/ρ for width, and (3) $E^{1/3}/\rho$ for height. These indices are derived for components with simple geometries and loads based on the classical elastic beam theory. For complex structures such as automotive body sub-assemblies, q may have values other than 1, 2 or 3 [12,13].

The mass ratio between beams made of two different materials for the same stiffness and design purpose [12] can be expressed by

$$R_{mass} = \frac{m_1}{m_2} = \frac{\rho_1/E_1^{1/q}}{\rho_2/E_2^{1/q}} \qquad (14)$$

where m is the mass, and subscripts 1 and 2 denote the two materials.

Fig. 2 shows the mass ratio by Eq. (14) for beams made of steel and aluminum for the same stiffness. For the material properties, refer to Table 1. It can be observed that the effect of weight reduction by aluminum substitution for steel is quite different with respect to different q values. At a larger q, aluminum can offer significant weight reduction. For small q values, aluminum leads to a minor weight reduction.

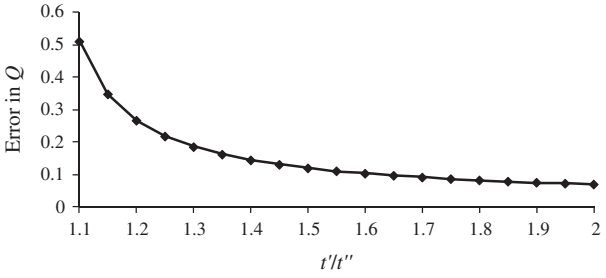

Fig. 1. The Q estimate deviation caused by a 5% error of F_m.

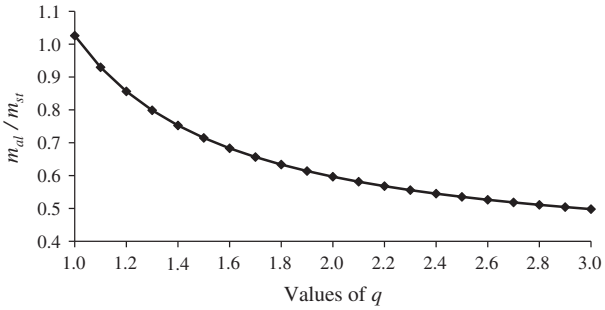

Fig. 2. Mass ratio between aluminum and steel versus q for the same stiffness. (Subscripts *al* and *st* denote aluminum and steel, respectively.)

Table 1
Material properties.

Material[a]	Elastic modulus (GPa)	Density (kg/m^3)	Price ($/kg)	σ_Y (MPa)	σ_U (MPa)
Mild	207	7840	0.80	180	300
BH	207	7840	0.85	210	500
DP	207	7840	1.1	450	800
Al 6063	70	2720	2.2	90	172
Al 6010	70	2720	2.4	170	290

[a] Mild (mild steel); BH (Bake-Hardenable); DP (dual phase); Al (aluminum).

3.2. Consideration of the mean crush load

From Eq. (9), the mass ratio between thin-walled beams made of two different materials for a constant mean crush load is

$$R_{mass} = \frac{m_1}{m_2} = \frac{\rho_1/\sigma_{f1}^{1/Q}}{\rho_2/\sigma_{f2}^{1/Q}} \qquad (15)$$

where m is the mass, subscripts 1 and 2 denote the two materials.

Fig. 3 shows the mass ratios for beams made of Bake-Hardenable (BH) high strength steel and aluminum alloy 6063 with respect to mild steel for a constant mean crush load. Properties of these materials are given in Table 1. It is interesting to see from Fig. 3 that the mass of the BH steel beam increases as the Q value increases, whereas the mass of the aluminum beam decreases. At a larger Q, aluminum seems to be a better choice, since it can achieve larger weight reduction. For small Q values, high strength steel can be preferred, since high strength steel offers a comparable weight reduction but can keep overall cost down.

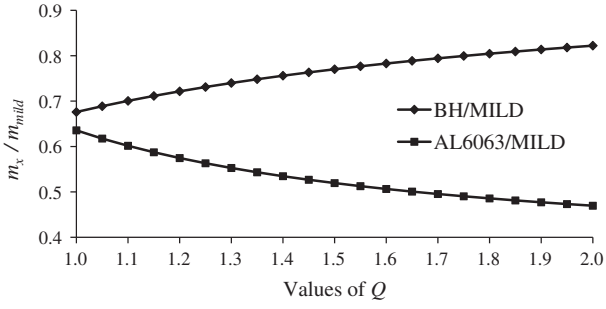

Fig. 3. Mass ratio of BH high strength steel and aluminum alloy 6063 with respect to mild steel as functions of Q for the same mean crushing load. (Subscript x denotes BH high strength steel or aluminum 6063.)

4. Cost evaluation model

Automotive bodies made of multiple materials should satisfy conflicting requirements such as minimum weight and minimum cost, while ensuring high rigidity and good crashworthiness. To handle these multi-objectives, this study employs a monetary value function, V, representing a composite objective value [23].

$$V = \alpha_1 m + C_m = \alpha_1 m + pm = (\alpha_1 + p)m \tag{16}$$

where m is the structural mass, C_m is the total material cost ($), α_1 is an exchange constant accounting for the change in value V with respect to unit increase in m, and p is the unit raw material price ($/kg). The values of the exchange constant relating mass and cost for family cars can be found in the literature, for example α_1 = (0.5–1.5) $/kg in [23]. The best design solution can be achieved by selecting materials that make the smallest V.

Substituting Eq. (9) into Eq. (16)

$$V = (\alpha_1 + p)\left(\frac{\rho}{\sigma_f^{1/Q}}\right)\left(\frac{F_m}{C}\right)^{1/Q} A \tag{17}$$

As mentioned in Section 2, $(F_m/C)^{1/Q}A$ is constant. Therefore, for a given crush load, the best material for crashworthiness-centered design is the one with the smallest value of

$$V_c = (\alpha_1 + p)(\rho/\sigma_f^{1/Q}) \tag{18}$$

Similarly, for stiffness-centered design, it is easy to derive that the best material is the one with the smallest value of

$$V_s = (\alpha_1 + p)(\rho/E^{1/q}) \tag{19}$$

Eqs. (18) and (19) can be used for individual components for crashworthiness and stiffness designs, respectively. Applying Eqs. (18) and (19) for all components, the optimization formulation for the whole car body can be defined conceptually for crashworthiness-centered design as follows.

$$\min z = \sum_j V_{c,j} \tag{20}$$

Subject to:

$$\begin{aligned} f_C(x_{11}, \ldots, x_{ij}, \ldots, x_{mn}) &\leqslant D_C \\ f_S(x_{11}, \ldots, x_{ij}, \ldots, x_{mn}) &\geqslant D_S \end{aligned} \tag{21}$$

$$\sum_i x_{ij} = 1, \quad \forall j \tag{22}$$

$$x_{ij} \in \{0, 1\} \tag{23}$$

Eq. (20) represents the objective function, in which term $V_{c,j}$ represents the value function of structure member j for crashworthiness. The value of variable x_{ij} is one if and only if material i is selected for member j, zero otherwise. Constraint Eq. (21) represents crashworthiness and stiffness conditions. D_c represents global crashworthiness criteria to be met by the whole car body, and D_S is the global stiffness requirement. f_C and f_S are crashworthiness and stiffness calculated by FE software for the whole car body. The constraint in Eq. (22) ensures unique material selection for each member. Constraint Eq. (23) expresses binary condition for the variables.

This problem is highly nonlinear because the calculation involves nonlinear FE simulations. Therefore, instead of traditional optimization methods, alternative approaches can be used. One approach is to use an iterative method. The value of min z is obtained first without considering the whole body crashworthiness and stiffness. Then for the material selection for each member, the f_C and f_S are checked if they satisfy the constraints. Then, the materials in the components are updated iteratively until feasible solutions are found. Another approach is to use approximation by dividing the components for mainly crashworthiness design or stiffness design. Many components are related to both crashworthiness and stiffness, but the knowledge on car body design can suggest each component's main contribution to either crashworthiness or stiffness. Then, f_C and f_S can be evaluated separately using each component groups. The detailed optimization methods and combination with other solution procedures [24] are beyond the scope of this paper and should be addressed in a future study, because the primary focus of this paper is the development of the material performance indices.

5. Case study

This section illustrates the application of the performance indices and material selection procedure for the design of lightweight automotive body structure.

5.1. Problem description

Optimal materials are selected for each primary structure frames to design the body as inexpensive and light as possible. The FE model of the car body is shown in Fig. 4. This FE model was obtained from the US National Highway Traffic Safety Administration (NHTSA) [25] with permission to use for research. Five candidate materials are considered and listed in Table 1. The body is originally made of mild steel (Mild) and Bake-Hardenable (BH) steel. The body structure has been decomposed into 20 primary structural components as shown in Table 2.

The frontal impact and global static bending stiffness of the car are considered for the material selection. The frontal impact was a simulated frontal collision against a rigid wall at the speed of

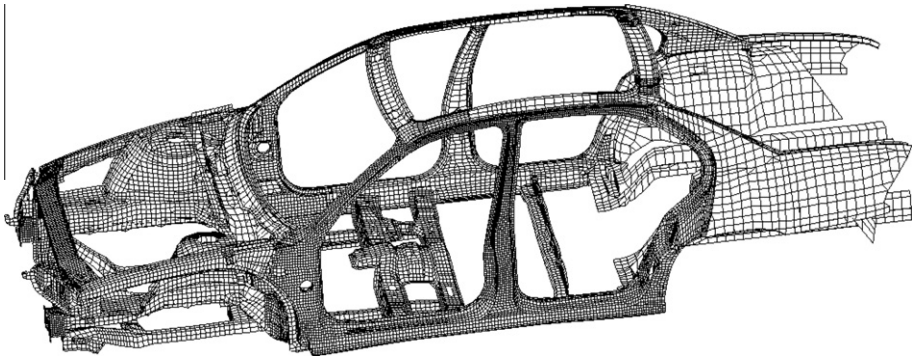

Fig. 4. Case study automotive body structure [25].

Table 2
Exponent values (Q and q) and materials selection in the primary members.

Primary structural member	Q and q[a]	Original design	Optimal design	Worst design
Cradle	1.28	BH	DP	DP
Upper rails	1.67	BH	Al 6010	Al 6010
Front rails	1.43	BH	DP	DP
Radiator support	1.21	Mild	Mild	Al 6063
Front shock towers	2.17	Mild	Al 6063	Mild
Instrument panel structure	1.61	Mild	Mild	Al 6063
Member front floor support	2.4	Mild	Al 6063	Mild
Front floor cross member	1.52	Mild	Mild	Al 6063
Front rail extensions	1.26	Mild	Mild	Al 6063
Hinge pillars	1.64	Mild	Mild	Al 6063
A-pillars	1.63	Mild	Mild	Al 6063
Front rockers	1.66	Mild	Mild	Al 6063
B-pillars	1.55	Mild	Mild	Al 6063
Roof rails	1.98	Mild	Al 6063	Mild
Rear rockers	1.52	Mild	Mild	Al 6063
C-pillars	1.84	Mild	Mild	Al 6063
Rear wheel houses and shock towers	2.27	Mild	Al 6063	Mild
Rear floor cross member	1.34	Mild	Mild	Al 6063
Rear rail extensions	1.82	Mild	Mild	Al 6063
Rear rails	1.23	Mild	Mild	Al 6063

[a] Values of cradle, upper rails and front rails are Q corresponding to crashworthiness design, and the other values are q corresponding to bending stiffness design.

48 km/h. This crash analysis was carried out by LS-DYNA®, an explicit dynamic FE code. For static bending stiffness analysis, four loads of 1000 N were applied at the front and rear seat mounts respectively. The rear shock mount was constrained in the longitudinal, lateral and vertical directions, and the front shock mount was constrained only in the vertical direction. The bending stiffness was evaluated as the average deflections at the load application points. The static bending analysis was performed by FEA software MSC/NASTRAN®.

5.2. Optimal material selection for primary members

The 20 primary structural components are divided into two groups according to their purposes. In the event of frontal collisions, the front side members including cradle, upper rails and front rails are the main elements designed to serve as energy absorbers. These three parts were chosen for material selection for crashworthiness design, and the other parts for bending stiffness design.

For the three main crash-energy absorbing components, the material performance indices as well as exponents Q were evaluated using Eq. (12) and FE analysis. The three front side members were simulated individually for colliding axially against a rigid wall with an initial velocity 48 km/h by FE analysis. In the FE models, a mass element is attached to one end of the structure to supply enough energy for crushing. The calculated Q values are listed in Table 2.

For the static bending stiffness case, the concept of the first-order analysis (FOA) [26] was employed to identify the local boundary and loading conditions for each primary frame. A beam-based FE model to represent the whole body structure was constructed first. In this model, the beam elements have the detailed cross-sectional information. Local boundary and loading conditions in bending for each primary member can be determined using the member forces and moments by the beam-based FE model. Table 2 shows the values of exponent q of performance indices for bending stiffness design, evaluated using a method in a study for car body stiffness [13].

Based on the calculated performance indices, optimal materials were selected for each primary member by using the smallest values of V_c and V_s in Eqs. (18) and (19) and the exchange constant $\alpha_1 = 1.5$ \$/kg. The optimal materials for all primary components are listed in Table 2. Note that in this case study the 'optimum' is related to only the V values for illustration purpose and the meaning of 'optimal' can be different in practice depending on objective function choices.

5.3. Verification of the material selection

To verify the performance of the car body with the optimal material selection, the whole vehicle's front crash simulations were performed for both the original body structure (all-steel body) and the optimal design adopting the material combination in Table 2. The thicknesses of the three front side members for crashworthiness design were determined using Eq. (7). Fig. 5 shows the crash deformation of car bodies for the original body design and the optimal design. It was observed that there is little difference in the overall deformed shapes of the two designs. Fig. 6 shows the total energy absorption of the three front side members for the original and optimal design. Although the difference was not significant, the optimal design showed better energy absorption than the original design. A comparison of the time history of the acceleration at B-pillar between the original and optimal design is given in Fig. 7. It was observed that the shapes of the acceleration curves, the peak magnitudes and average decelerations for the two cases were not significantly different.

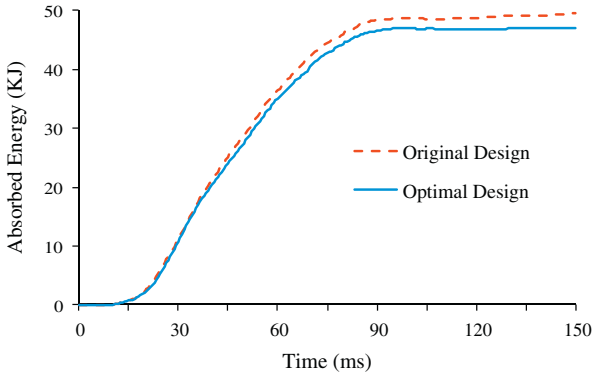

Fig. 6. Energy absorption of the front side members for the original and optimal design.

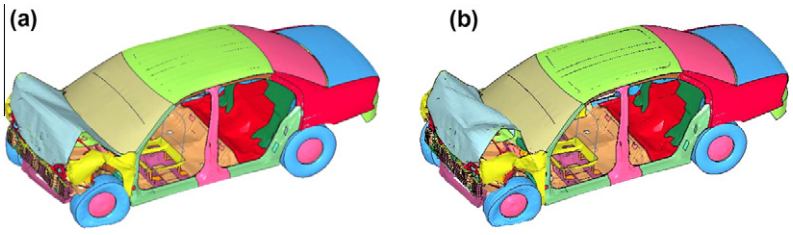

Fig. 5. Crash deformation of car bodies: (a) original body design and (b) optimal design.

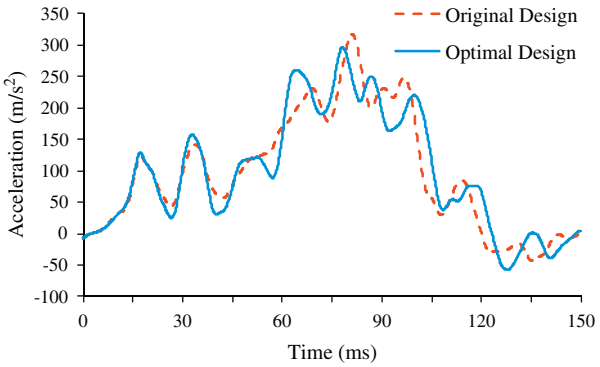

Fig. 7. Acceleration at B-pillar versus time.

The optimal material selection was also verified for the global bending stiffness by FE bending stiffness simulations carried out for both the original and optimal material selections. The results of bending stiffness analysis indicated that the stiffness of the optimal design was very close to that of the original body design. The bending deflections of the two body material selections were 1.57 mm and 1.66 mm respectively.

To further verify the methodologies in the study, the worst material selection case was also examined. The materials were selected with respect to the largest values of V_s in Eq. (19), except the three main crush-energy absorbing components. The bending deflection of this worst design is 1.43 mm. Although the worst design is slightly stiffer than the original body design, the difference was marginal.

6. Discussion

This section discusses the results and effectiveness of the multi-material selection for the lightweight automotive body structure.

6.1. Optimal multi-material car body

The case study results demonstrate that the use of the developed methodologies led to a new design superior to the original design. As demonstrated in Section 5.3, the optimal material replacement is at least as good as the original material selection in terms of crashworthiness performance. The bending stiffness of the optimal design is also very similar to that of the other body designs. All these performance values were achieved with much less weight and cost values.

To compare the different designs in more detail, the designs were updated for equivalent bending stiffness. Several components' thicknesses were slightly modified for both the optimal and worst body designs so that the two bodies have an equivalent bending stiffness to the original body design. Table 3 compares the structural weights, material costs and V values for the original and the updated optimal and worst body designs. As can be seen from Table 3, the optimal multi-material body achieved weight reduction of 30.9 kg with only $14.3 material cost increase. This optimal design led to a lightweight and cost-effective body assembly that can provide high fuel economy and affordability. The worst design in terms of V led to 64.6 kg weight reduction from the original design but the material cost increased by $132.8. This is due to the extensive use of lightweight but expensive aluminum alloys. As shown by these comparisons, these different designs can lead to quite different product performance.

Table 3
Performances comparison of body designs with equivalent bending stiffness.

Body structures	Bending stiffness[a] (mm)	Weight (kg)	Cost ($)	V value ($)
Original design	1.5744	236.3	191.2	545.6
Optimal design	1.5735	205.4	205.5	513.6
Worst design	1.5739	171.7	324.0	581.6

[a] The bending stiffness was evaluated as the deflection at the load application point under the fixed load.

6.2. Effectiveness of the developed indices and process

The case study results also demonstrate that this study provides efficient procedures and formulas for multi-material car bodies [8–10] and enhance existing material selection methods.

First, the developed indices allowed evaluating the advantages and disadvantages of different materials in complex-shape structure. In particular, the indices can consider crashworthiness performance easily. This was possible by using the new material performance indices for crashworthiness by Eq. (10) and calculating the exponent in Eq. (10) easily using FE-simulation based procedures. These new indices and calculation procedures expand the scope of the previous studies on stiffness [12,13] and simple structures to including the crashworthiness of complex beams.

Second, the developed cost evaluation methods allowed achieving the best lightweight and cost-effective design of automotive bodies under stiffness and crashworthiness constraints. The case study results showed that equivalent-performance car bodies were constructed with significant weight reduction around 30 kg and less material cost. This was possible by the use of the systematic cost evaluation methodologies shown in Section 4. Therefore, the developed procedure can be used to overcome the material price problem, one of the principal barriers to replacing steel-based structure for fuel efficiency [7]. Through optimal material selection for each primary structural member, there is a good chance to fully utilize the advantages of each material and achieve the optimal product performance. The car bodies designed such a way will appeal to the customers and manufactures because of the affordability due to the light weight materials used only on the right places.

7. Conclusions

This paper developed novel material performance indices of thin-walled structural parts for crashworthiness design. These new performance indices enable to characterize complex-shape structural components in automotive bodies in terms of mechanical performance and material costs according to material types. Thus, the indices allow us to select optimal materials for the structural parts systematically. Furthermore, the indices were developed for convenient evaluation and use. The case study demonstrated that the new indices helped to achieve a substantial material cost reduction with comparable product performance or considerable weight reduction without significant cost increase.

This study shows that, through multi-material construction and the optimal materials selection for each structural member in automotive bodies, lightweight and high structural performance can be accomplished without substantial material cost increase. These new indices enable to design such a lightweight and affordable body favored by the automotive industry and consumers, and will help to reduce fuel consumption and greenhouse gas emissions.

In a future study, fabrication processes can also be considered for an automotive body of multi-material construction. These considerations can be implemented by taking into account technical

and economic aspects of forming and joining processes. For example, joining dissimilar material may lead to more costly processes or equipment. These extensions are worth further investigations.

References

[1] Han HN, Clark JP. Lifetime costing of the body-in-white: steel vs. aluminum. JOM 1995;47(5):22–8.
[2] Koehr R. Ulsac-lightweight steel automotive closures. SAE technical paper, paper no. 2001-01-0076; 2001.
[3] Li Y, Lin Z, Jiang A, Chen G. Use of high strength steel sheet for lightweight and crashworthy car body. Mater Des 2003;24:177–82.
[4] Deb A, Mahendrakumar MS, Chavan C, Karve J, Blankenburg D, Storen S. Design of an aluminium-based vehicle platform for front impact safety. Int J Impact Eng 2004;30:1055–79.
[5] Carle D, Blount G. The suitability of aluminium as an alternative material for car bodies. Mater Des 1999;20:267–72.
[6] Li Y, Lin Z, Jiang A, Chen G. Experimental study of glass-fiber mat thermoplastic material impact properties and lightweight automobile body analysis. Mater Des 2004;25:579–85.
[7] Kelkar A, Roth R, Clark J. Automobile bodies: can aluminum be an economical alternative to steel? JOM 2001;53(8):28–32.
[8] Jambor A, Beyer M. New cars–new materials. Mater Des 1997;18:203–9.
[9] Hahn O, Kurzok JR, Timmermann R. Joining of multi material constructions. In: Chinese–German ultralight symposium. Beijing, China; 2001.
[10] Cui X, Wang S, Hu SJ. A method for optimal design of automotive body assembly using multi-material construction. Mater Des 2008;29(2):381–7.
[11] Ashby MF. Materials selection in mechanical design. Butterworth-Heinemann; 2005.
[12] Patton R, Edwards M. Estimating weight reduction effects of material substitution on joints with constant stiffness. SAE technical paper, paper no. 2002-01-0386; 2002.
[13] Patton R, Li F, Edwards M. Causes of weight reduction effects of material substitution on constant stiffness components. Thin Wall Struct 2004;42:613–37.
[14] Farag MM. Materials selection for engineering design. Prentice Hall; 1997.
[15] Sapuan SM. A knowledge-based system for materials selection in mechanical engineering design. Mater Des 2001;22(8):687–95.
[16] Ermolaeva NS, Castro MBG, Kandachar PV. Materials selection for an automotive structure by integrating structural optimization with environmental impact assessment. Mater Des 2004;25(8):689–98.
[17] Ermolaeva NS, Kaveline KG, Spoormaker JL. Materials selection combined with optimal structural design: concept and some results. Mater Des 2002;23(5):459–70.
[18] Rossi A, Fawaz Z, Behdinan K. Numerical simulation of the axial collapse of thin-walled polygonal section tubes. Thin Wall Struct 2005;43:1646–61.
[19] Wierzbicki T, Abramowicz W. On the crushing mechanics of thin-walled structures. J Appl Mech 1983;50:727–34.
[20] Guillow SR, Lu G, Grzebieta RH. Quasi-static axial compression of thin-walled circular aluminium tubes. Int J Mech Sci 2001;43:2103–23.
[21] Lu G, Yu TX. Energy absorption of structures and materials. Woodhead Publishing Limited; 2003.
[22] Al Galib D, Limam A. Experimental and numerical investigation of static and dynamic axial crushing of circular aluminum tubes. Thin Wall Struct 2004;42:1103–37.
[23] Ashby MF. Multi-objective optimization in material design and selection. Acta Mater 2000;48:359–69.
[24] Jiang Z, Gu M. Optimization of a fender structure for the crashworthiness design. Mater Des 2010;31(3):1085–95.
[25] US national highway traffic safety administration. <http://www-nrd.nhtsa.dot.gov/> [accessed in 2007].
[26] Nishiwaki S, Nishigaki H, Amago T, Kojima Y, Kikuchi N. First order analysis-new cae tools for automotive body designers. SAE technical paper, paper no. 2004-01-0768; 2001.